

# Weather Type Classification and Its Relation to Precipitation over Southeastern China

Yongdi Wang,<sup>a,\*</sup> Xinyu Sun<sup>b</sup>

<sup>a</sup>*School of Remote Sensing and Geomatics Engineering, Nanjing University of Information Science and Technology, Nanjing, China*

<sup>b</sup>*Key Laboratory of Meteorological Disaster, Ministry of Education (KLME) / Joint International Research Laboratory of Climate and Environment Change (ILCEC) / Collaborative Innovation Center on Forecast and Evaluation of Meteorological Disasters (CIC-FEMD) / Jiangsu Key Laboratory of Meteorological Observation and Information Processing / Jiangsu Technology & Engineering Center of Meteorological Sensor Network, Nanjing University of Information Science and Technology, Nanjing, 210044, China*

*Corresponding author: Yongdi, Wang Contact: [ydwang@nuist.edu.cn](mailto:ydwang@nuist.edu.cn)*

**ABSTRACT:** It is very important to identify the possible mechanism of precipitation generation in southeastern China. To determine the weather type (WT) that is likely to generate precipitation, the Jenkinson-Collison (JC) classification method was applied to wintertime daily mean sea level pressure (MSLP) data across southeastern China. We found that all WTs with easterly components are prone to generate precipitation. These WTs were merged into one type named the ensemble of easterly wind components (the EE type). The persistence and transformation rules of the EE type are studied. Anticyclone type is the easiest one to convert to EE type. The persistence and transformation rules of the EE type provide favorable conditions for the formation of precipitation. Furthermore, we examined the influence of two common teleconnections (Western Pacific (WP) and Eurasian (EU)) in East Asia in winter on the WTs. When WP is in the positive phase and EU is in the negative phase, EE type

This article has been accepted for publication and undergone full peer review but has not been through the copyediting, typesetting, pagination and proofreading process which may lead to differences between this version and the Version of Record. Please cite this article as doi: 10.1002/joc.6747

weather patterns will appear frequently in southeastern China. At this time, it is most conducive to the formation of precipitation. On the one hand, warm and cold air converge in this area. On the other hand, the prevailing east wind can provide sufficient water vapor. The study implies that whether a weather type is easy to produce precipitation can be judged by wind direction. The results will help us better understand the physical mechanism of precipitation generation in this area.

**KEY WORDS** Weather type; Synoptic climatology; Southeastern China; Jenkinson-Collison synoptic classification; Teleconnections; Precipitation

## 1. Introduction

In recent years, extreme weather and climate events have been attributed to accelerated climate change. An increasing number of recent studies have begun to uncover the physical bases of the intensifying weather and climate fluctuations in a warming climate. Extreme weather and climate events can be related to specific atmospheric circulation patterns. Therefore, studies of regional climate change (extreme weather and climate events) are often linked to variations in atmospheric circulation (Yarnal *et al.*, 2001).

Synoptic climatology has become an important tool for the classification of weather types (WTs), which has been proven to be powerful and effective in practice (Sarricolea *et al.*, 2018; Jiang *et al.*, 2015; Huth *et al.*, 2016). One of its basic tasks is establishing the relations between atmospheric circulation and local weather (Yarnal *et al.*, 2001). To facilitate analysis, the continuum of atmospheric circulation can be simplified into a reduced number of representative categories (Huth *et al.*, 2016). Each type represents a weather pattern or a WT. With this method, we can use the approach to describe the main WTs in a given region and identify the causes of regional climate change. For example, atmospheric variability can be studied by analysing the variations in frequency of specific WTs (Huth, 2000; Jiang *et al.*, 2012a). By analysing the relationship between WTs and teleconnections, we can better understand the atmospheric conditions on a larger scale (Jiang, 2011; Jiang *et al.*, 2012b). These studies will contribute to an improved understanding of the relationship

between various patterns and teleconnections and the influence of teleconnections on these patterns (Roller *et al.*, 2016). Studying the conversion between weather patterns is beneficial to understanding the evolution law of weather and the underlying physical causes. In particular, atmospheric circulation is the driving force of precipitation variability (Post *et al.*, 2002; Riediger and Gratzkil, 2014). The variation in WT can provide valuable information for the study of surface variables. For example, atmospheric circulation changes can reduce or exacerbate precipitation changes (Belleflamme *et al.*, 2015).

Classification is a common method for studying atmospheric circulation. Among many classifying techniques, one of the common methods is the Jenkinson-Collison (hereinafter JC) synoptic classification method (Jenkinson and Collison, 1977). This classification method improved the Lamb WT (Lamb, 1972) system and was initially used in the British Isles region (Spellman, 2017). The results of Jones *et al.* (1993) show that this method can effectively replicate the Lamb WTs. This method has many advantages, e.g., the method is very operable, requires less input data, has a clear physical meaning (easy to explain its formation mechanism), and is suitable for different latitude regions (any mid- to high-latitude region) (Jones *et al.*, 2013; Donat *et al.*, 2010; Otero *et al.*, 2017). Therefore, this method has been used in a wide range of applications, including providing the contents of dynamic analysis (Straus *et al.*, 2007; Moron *et al.*, 2008; Qian *et al.*, 2010) and the basis of downscaling (Conway and Jones, 1998; Moron *et al.*, 2008; Demuzere *et al.*, 2009), evaluating the trend and prediction of weather changes (Riddle *et al.*, 2013), and providing a basis of model evaluation (Perez *et al.*, 2014). The continuity and transformation of WTs can also be applied to seasonal change and prediction analysis, thereby linking the weather to the climate (Coleman and Rogers, 2007).

The classification results can provide a basis for the subsequent analysis. If we want to better understand the physical mechanism of precipitation generation on a larger scale, we need to consider several atmospheric teleconnection patterns that are common in winter. To better comprehend the relationship between WTs and larger-scale circulation, the relationships between each WT and

several important climatic teleconnection types are investigated. Wallace and Gutzler (1981) found that there are five teleconnection patterns among the 500 hPa geopotential height anomalies over the winter northern hemisphere: Eastern Atlantic (EA), Pacific-North American (PNA), Western Atlantic (WA), Western Pacific (WP) and Eurasian (EU). The EU and WP teleconnection patterns have a very important impact on the winter climate in China and East Asia, especially temperature and precipitation (Shi, *et al.*, 1995). Li and Chou (1990) proposed that the EU teleconnection pattern is the main factor of the anomalous winter precipitation in the middle and lower reaches of the Yangtze River. The change in EU teleconnection pattern in winter is closely related to the general circulation in East Asia (Liu and Chen, 2012). The WP teleconnection pattern in winter has a significant positive correlation with winter precipitation in China (Li *et al.*, 2007). It appears that the WP and EU teleconnection patterns all have closer links to Chinese winters, which echoes earlier research (Shi *et al.*, 1995). Therefore, our analysis focuses on the relationship between WTs and these two teleconnections (WP and EU).

The factors that affect precipitation are complex. Because the state of each meteorological element needs to be comprehensively analysed, it is difficult to judge whether a region will form precipitation from the perspective of weather type. If the formation of precipitation can be judged according to the prevailing weather type, it will bring great convenience to people's production and life. Taking all of the abovementioned considerations into account, this paper has a few purposes. First, in order to judge which weather type is easy to produce precipitation simply according to the wind direction, we identify the WTs that are most conducive to precipitation generation, and combine them into a new type. To do this, we use the JC classification method to obtain the winter WTs in southeastern China, to judge the applicability of this method in the region and to provide a basis for the following analysis. Second, our goal is to better understand its internal physical mechanism. For this reason, we investigate the persistence and transformation rules of the most frequent types, and examine the influence of several common teleconnections in East Asia in winter

on the WTs. This approach will help us better comprehend the mechanism of precipitation generation on a larger scale.

## 2. Data

The National Center for Atmospheric Research (NCEP) - U. S. Department of Energy (DOE) AMIP-II NCEP-DOE Reanalysis II or NCEP2 is provided by the National Centers for Environmental Prediction/National Center for Atmospheric Research (NCEP/NCAR). The data is an improved version of NCEP-NCAR reanalysis I. The NCEP2 covers the 20-year satellite period from 1979 to the present and uses an updated forecast model, updated data assimilation system, improved diagnostic outputs, and resolves the known NCEP-NCAR reanalysis processing problems (Kanamitsu *et al.*, 2002).

In this paper, to classify WTs, the NCEP2 reanalysis daily mean sea level pressure (MSLP) at a  $2.5^{\circ} \times 2.5^{\circ}$  regular (latitude/longitude) resolution for December-February (DJF) from 1979-2005 are used as input for the JC classification method. For the purpose of characterizing the resulting WTs, 27 years (1979-2005) of the NCEP2 reanalysis daily 850-hPa zonal  $u$  and meridional  $v$  component winds ( $2.5^{\circ} \times 2.5^{\circ}$ ) are also used for DJF. In the teleconnection analysis, the NCEP2 reanalysis daily 500-hPa geopotential height dataset was selected to calculate teleconnection indices following Wallace *et al.* (1981).

In addition to the reanalysis data, the gridded precipitation data provided by Chen *et al.* (2010) have also been used (referred to as CHEN05). The data resolution is  $0.5^{\circ}$  by  $0.5^{\circ}$ . This dataset is also obtained from 753 operational surface stations of the China Meteorological Administration by

ordinary kriging interpolation, with small interpolation errors in the eastern part of China owing to the high station density.

### **3. Methods**

#### **3.1. Analysis domains**

Analysis is performed on two regions: a large domain (bounded by 20°-50°N latitude and 100°-130°E longitude), equivalent to the original area size of the original catalogue, was defined (Jenkinson and Collison, 1977; Jones *et al.*, 1993), which covers southeastern China, and a small domain (bounded by 25°-35°N latitude and 110°-120°E longitude), occupying the core of the large domain (Figure 1). Among these domains, the larger domain is used to calculate the JC classification input, and the smaller domain is used to conveniently calculate the precipitation index (defined in the latter part).

Figure 1. Map showing the boundaries of southeastern China used for JC classification and the core domain (the rectangle inside the larger rectangle). The 16 grid points generated via a distribution algorithm around the central point (square) located in southeastern China were likewise plotted.

#### **3.2. Classification of the WT**

According to the definition of the original method (Jenkinson and Collison, 1977; Jones *et al.*, 1993), gridded daily MSLP data are interpolated to a 16-point grid (p1-p16). For a given day, its circulation pattern is determined according to the locations of the centres of high and low pressures that determine the geostrophic airflow direction. Successfully identifying the circulation pattern depends on whether the JC classification is successful. The analysis includes the strength and direction of airflow and the type of baric system (cyclonic or anticyclonic). Through classification, 27 types can be obtained. Among these types, there are 8 directional types, 2 rotational types, 16

Accepted Article

mixed types and 1 unclassified type. Unclassified denotes a type of weak or chaotic flow, which in the following is referred to as the low flow (LF) type. According to the research results of Jones *et al.* (2013), Donat *et al.* (2010) and Otero *et al.* (2017), we know that JC method can be applied to any middle and high latitudes. Therefore, it should also be applicable in southeastern China. But this method was designed to study the British Isles, and the wind resources in southeastern China are far less abundant than those in Europe, so the setting of threshold parameters has been changed (LF type threshold changed from 6 to 1). Therefore, after modification, the proportion of LF in the classification results was changed to 0.

### 3.3. Precipitation characterization

To further characterize the precipitation associated with the WTs, the daily and extreme precipitation levels are examined using the daily gridded dataset mentioned before. The CHEN05 grid data are used to calculate daily and extreme precipitation characteristics. The daily precipitation characteristics are evaluated at each grid point. The number of precipitation days ( $>0.1$  mm), the daily intensity on precipitation days, and the total precipitation were calculated following Agel *et al.* (2015). The CHEN05 grid dataset is also used to calculate the extreme precipitation (defined as the top 1% of the daily intensity on precipitation days). The mean number of extreme precipitation days, the daily intensity on extreme precipitation days, and the total extreme precipitation for each WT were calculated.

### 3.4. Calculation of the teleconnection patterns

Teleconnection may influence wintertime weather over southeastern China. By investigating the relationship between each WT and several important teleconnections, we can better understand the link between the WTs and large-scale circulation regimes. Here, we selected two teleconnection patterns that have a very important impact on the winter climate in China and East Asia. One teleconnection pattern is the WP pattern, and the other teleconnection pattern is the Eurasian (EU)

pattern. Following Wallace *et al.* (1981), we determined these two teleconnections. The two teleconnection indices were defined as follows:

$$WP = \frac{1}{2}[Z^*(60^\circ\text{N},155^\circ\text{E}) - Z^*(30^\circ\text{N},155^\circ\text{E})] \quad (1)$$

$$EU = -\frac{1}{4}Z^*(55^\circ\text{N},20^\circ\text{E}) + \frac{1}{2}Z^*(55^\circ\text{N},75^\circ\text{E}) - \frac{1}{4}Z^*(40^\circ\text{N},145^\circ\text{E}) \quad (2)$$

where  $Z^*$  are the normalized 500-hPa height anomalies at specified grid points corresponding to centres of action or antinodes of the pattern. Further details about the calculation procedure for these teleconnection indices can be found in Wallace *et al.* (1981).

## 4. Results and discussion

### 4.1 Weather types

Zhu *et al.* (2007) used this method to divide China into 16 regions to study the classification of regional atmospheric circulation of China. Then they discussed the applicability of this method of China. The results show that different circulation patterns can be clearly distinguished from different regions of China by using this method, which shows that this method is applicable to most regions of China. This method has a good application prospect of regional climate analysis, prediction and change research in China. The research area selected in this paper is basically consistent with the sixth area divided by Zhu *et al.* (2007). It shows that the weather classification results of this paper are effective and can be reproduced.

The data were separated into 27 types, with each day assigned to a single type. Each type represents a WT. Comprehensive views of the classification results are shown in Figures 2 (MSLP anomalies) and 3 (precipitation and wind anomalies).

Figure 2. Weather types: mean sea level pressure (MSLP) anomalies (contour; hPa) for winter (DJF) 1979-2005. The subgraphs are ranked from high to low according to the frequency of occurrence. The frequency (F) of each

class is also shown in brackets in the subgraphs. The MSLP anomalies were calculated by subtracting the averaged MSLP over the 27-yr baseline period from the daily MSLP at each grid point for the NCEP2 MSLP data.

The subgraphs are ranked from high to low according to the frequency of occurrence (Figure 2). The frequency (F) of each class is also shown in brackets in the subgraphs. In winter, the frequency proportions of the various WTs are very uneven. Certain WTs, including anticyclone components, occur relatively frequently (e.g., AE, ASE, and ANE). Among these WTs, the anticyclone type (F = 56.54%) has the highest frequency. In contrast, the WTs with cyclonic components have a relatively low frequency (e.g., CE, CSE, and CSW). Among these WTs, the highest frequency does not exceed 2%, such as the cyclone (C) type, whose frequency is 1.85%. In addition, there are two WTs (N and LF) whose frequencies are zero, which are not shown in the figures.

Figure 3. Precipitation and wind patterns derived from the weather types (corresponding to Figure 2): precipitation (PR) (shaded; mm/d) and 850 hPa wind anomalies (vectors) for winter (DJF) from 1979-2005.

In winter, cyclone types are rare (1.85%). Precipitation mainly occurs as frontal rain. The cold and warm two-stream intersection and enough moisture are the two indispensable conditions of precipitation generation. If the two conditions are satisfied at the same time, the probability of precipitation is high; otherwise, the probability of precipitation is low. For example, the pressure fields of the easterly wind type (Figure 2 (c)) and the westerly wind type (Figure 2 (p)) meet the convergence conditions of cold and warm air. The easterly wind type is low in the south and high in the north, while the westerly wind type is low in the north and high in the south. However, because of the opposite wind directions, these wind types can transport water vapour with completely different abilities. The easterly type can bring enough water vapour from the eastern ocean (Figure 3 (c)), while the westerly type cannot carry water vapour (Figure 3 (p)). Because the easterly wind type satisfies the precipitation generation conditions, precipitation occurs (Figure 3 (c)).

## 4.2 Reorganization of the WTs

### *a. Ranking of the various precipitation indicators and analysis of their characteristics*

To determine the WTs that are most likely to generate precipitation, we examined the daily precipitation and extreme precipitation across southeastern China. From Figure 4, it is clear that the number of precipitation days and precipitation intensity differ between the WTs (Figures 4 (b) and (d)). The total amount of precipitation depends largely on the frequency and intensity of precipitation. For example, the total amount of precipitation in the anticyclone (A) type is the largest, and the precipitation intensity in this type is very low (not in the top 10), while the frequency of occurrence of this anticyclone type is the highest. In contrast, the precipitation intensity of CNE is very high, but the CNE type has a low frequency of occurrence of (not in the top 10).

Most extreme precipitation occurs in the easterly (E) and anticyclone (A) types (Figure 4 (h)), with no extreme precipitation associated with N, CN, AN, W, CW, AW, NW, ANW or CNW (not shown). This phenomenon means that although the north or west wind components are strong, the occurrence of extreme precipitation is almost impossible. Overall, the types that easily generate extreme precipitation can be divided into three categories. The first category has more precipitation days and a higher total but less intense precipitation (e.g., E and A). The second category has fewer precipitation days and a lower total but more intense precipitation (e.g., ANE, and S). The rest fall into the third category (e.g., NE and AE). Large amounts of precipitation can also be generated in this category. The frequencies and intensities of this category are neither low nor high in the ranking results. It should be noted that most of the above three categories contain easterly wind components. This result is consistent with Li *et al.* (2007).

Figure 4. Mean precipitation characteristics (top 10) in the core domain for winter (DJF) from 1979-2005.

### *b. The WTs most likely to generate precipitation and the re-combination of the WTs*

After the statistics of the top10 of each index, the next step is to select the most precipitation-prone WTs on this basis. We redivide and combine these WTs according to the wind direction, including six different categories (east, west, north, south and two rotation directions). Then, the number of times each of the six new categories appeared in the top10 of each indicator in Figure 4 is counted. We think that more times appearing type was more conducive to precipitation generation. We consider that a combination that is most likely to generate precipitation would appear more frequently in the top 10 of all precipitation indicators, which are listed in Table 1.

The WTs with easterly components appear most frequently in eight subgraphs (expressed in bold). The results show that the WTs with significant impacts on the positive precipitation anomalies in winter are mainly the 9 easterly wind-related types (ANE, NE, CNE, AE, E, CE, ASE, SE, and CSE), which in the following, we refer to as the ensemble of easterly wind components type (hereafter simply the EE type).

From the above analysis, we can deduce that the types related to the easterly wind components are the most likely to produce precipitation or extreme precipitation in winter. The types associated with northerly or westerly wind components hardly produce precipitation in winter. This phenomenon can be explained as follows. In the winter, southeastern China is dominated by high pressure. Dry and cold airflows are the main airflows across the continent. Once a warm and wet airflow enters, the airflow will meet the conditions of precipitation generation. Both the north and west winds blow from land to ocean. These winds are dry and cold and will not carry moisture. In contrast, the type related to the easterly component is blowing from ocean to land and will bring a warm and humid airflow. This situation is very conducive to precipitation generation. These easterly wind-related types can bring warm and humid airflows. Therefore, these WTs have significant impacts on positive precipitation anomalies.

Table 1. Number of top 10 occurrence of each classification in sorting results according to different precipitation indexes. The maximum value is expressed in bold.

Furthermore, we can also observe a significantly positive correlation (at the 95% confidence level) between the occurrence frequency of the EE type and precipitation ( $r=0.62$ ) (year-by-year sequential calculation). Therefore, it may be possible to predict the change in precipitation by changing the frequency of the EE type. From the above analysis, we can also observe that the WTs that affect precipitation are often not a single WT but several WTs (e.g., the EE type). It is found that the weather patterns with an easterly component (i.e., AE, E, ASE, SE, ANE, NE, CSE, CE and CNE) are often the ones that can bring large precipitation (Figure 3(b), (c), (d), (e), (f), (g), (k), (j) and (o)). And it is easier to bring precipitation than the corresponding pattern of a westerly component (i.e., AW, W, ASW, SW, ANW, NW, CSW, CW and CNW) (Figure 3(w), (p), (r), (m), (v), (t), (n), (u) and (y)). For example, E type is easier to produce precipitation than W type, AE type and CE type are easier to produce precipitation than AW type and CW type respectively. Their common feature is that these WTs all contain easterly wind components. The wind from an easterly direction can always transport water vapour and produces much precipitation. Proper classification method is the basis for obtaining correct analysis results. JC method has clear physical meaning and reasonable classification results, which is very helpful for our later analysis.

#### 4.3 Persistence and progression of the WTs

After classifying and recombining the WTs, another important task is to investigate the persistence and progression of the WTs (Coleman *et al.*, 2007). Due to the high frequency of EE type, even if the rain is always light in everyday in EE type, the total rainfall brought by EE type is still very large. Therefore, the analysis of the two aspects of persistence and progression rule can help us better understand why the EE type can produce a large amount of precipitation.

##### *a. Persistence*

The persistence of the WTs (the top 10 of the frequency rankings) is plotted in Figure 5. The frequency of each WT is marked on the subgraph title. Although most of the types will continue,

the same type usually does not last long. In winter, the duration of the anticyclone can be very long and last up to 25 days (Figure 5 (a)).

According to the above analysis, the WTs with significant impacts on positive precipitation anomalies are the 9 types related to the easterly components in winter (the EE type). The duration of the EE type is plotted in Figure 5 (b). Only 39.4% of the winter days persist in the EE type for 4 or more days. Only 27.0% of the winter days persist in the EE type for 5 or more days. The proportion of 1-3 days was significantly higher than the proportion of longer than 3 days. The duration of the remaining WTs is significantly shorter (Figures 5 (c)-(f)). In particular, the AS and SW types have only 1-day durations.

Figure 5. Persistence of WTs (a) A, (b) EE, (c) C, (d) S, (e) AS, and (f) SW (in winter), expressed as a percentage of the total WT days, for a duration of 1-25 days. The weather types that occur less frequently (frequency<0.5%) are not shown.

The possible explanation can be drawn from the dominance of high-pressure systems in winter. The occurrence of the easterly type is due to the temporary weakening of the high-pressure system. When the high-pressure system across Siberia is being rebuilt, the system will force the various weather patterns to switch back to the anticyclone type. Consecutive A-type days may be due to the high-pressure system across northern China that is associated with a strong low-level jet bringing cold northwesterly air into China, which results in a stalled high-pressure system. Consecutive EE-type days may be due to the weakened high-pressure system near the region, which allows warm moist air to enter the region from the east. The precipitation process often requires a certain duration. Although the duration of the EE type is not the longest, the EE type also has a certain persistence. This characteristic of the EE type is more conducive to precipitation generation.

*b. Progression*

Figure 6. Graphical representation of the progression and persistence of the top 10 WTs.

Figure 6 shows the progression and persistence likelihood (expressed as percent) of each WT. The EE type is formed by merging all the types that contain the easterly component, while the other types remain unchanged. The total number of WTs decreased from 27 to 19. The top 10 with the highest frequency are A (56.54%), EE (37.08%), C (1.85%), S (1.28%), AS (0.62%), SW (0.53%), CSW (0.33%), W (0.25%), CS (0.25%) and ASW (0.25%). Type A is most likely to persist as type A (998 times) or transition into type EE (294 times), and type EE is most likely to persist as type EE (518 times) or transition into type A (363 times). Type C is most likely to transition into type EE (34 times) or persist as type C (6 times), and type S is most likely to transition into type EE (18 times) or type C (10 times). Since type EE is often able to generate precipitation, we are concerned with the EE type. The EE type shows a high propensity for recurrence (57.5%) but can also transition into type A (40.3%). In addition, types C and S may also transition into type EE (75.6% and 58.1%, respectively), and type A transitions into type EE slightly less frequently (21.4%).

These findings suggest that the anticyclone type can easily be transformed into the EE type. In addition, the frequency of the anticyclone type is very high, so the probability of EE occurrence increases. Together, these favourable factors create conditions for the occurrence of EE and the generation of precipitation.

#### 4.4 Relationship between the WTs and teleconnections

The teleconnection analysis was performed by taking the daily WP and EU phases, as well as the WT assigned to each day, and determining the relative WT frequency for each teleconnection phase (positive ( $\text{index} > 1$ ), neutral ( $-1 \leq \text{index} \leq 1$ ) and negative ( $\text{index} < -1$ )) (Roller *et al.*, 2016). The frequency of the top 3 types during the various phases of the two climate teleconnections (WP and EU) are evaluated (Figure 7).

In Figure 7 (a), the frequency of each WT during the various WP phases was plotted. During the positive WP phase ( $\text{WP} > 1$ ), the occurrence of EE increases while the occurrence of A decreases.

During the negative WP phase ( $WP < -1$ ), the occurrence of A increases while the occurrence of EE decreases.

Figure 7. WT occurrence frequency during positive (+), neutral (~) and negative (-) phases of (a) WP and (b) EU in winter. For each WT, the three bars represent the occurrence frequency during the three phases of the teleconnection pattern. Each bar represents the percentage of the same phase of each teleconnection. The frequencies of the other WTs are particularly low and are not shown in the figure. For each WT, the three bars represent the frequency during the three phases of the teleconnection pattern. Each bar represents the percentage of the same phase of each teleconnection.

The large-scale circulation field results in a notable difference between the positive and negative WP phases. In the positive WP phase, a negative height anomaly persists across the Asian continent high latitude (Li *et al.*, 2007). The meridional pressure gradient is higher, the middle latitude westerly wind is stronger, the polar front area is in the north, and the circulation is zonal. Corresponding to these conditions, the Siberian high-pressure system is weak at the sea-level pressure field, and the East Asian winter wind is weak (Li *et al.*, 2007). The situation is the opposite in the negative WP phase.

In the positive WP phase, there is an anticyclonic circulation across Taiwan in China. The eastern part of China is located on the west side of the anticyclonic circulation, which is conducive to warm and humid air coming to the east coast of China. This phenomenon is the reason for the excessive precipitation. In the negative WP phase, the anticyclonic circulation centre has reached the southern China area. The warm and wet air at sea does not easily reach the eastern part of China, resulting in less precipitation. In addition, the circulation anomaly also corresponds to the relative humidity. In the positive WP phase, the relative humidity in eastern China has a positive anomaly. The largest anomalous centre is located in southern China, which is a favourable condition for this

area to experience more precipitation. In the negative WP phase, the eastern area has a negative humidity anomaly, which is not conducive to precipitation in this area.

In Figure 7 (b), the frequency of each WT during the various phases of the EU is plotted. During the positive EU phase ( $EU > 1$ ), the occurrence of A increases while the occurrence of EE decreases. During the negative EU phase ( $EU < -1$ ), the occurrence of EE increases while the occurrence of A decreases. Type S only appears in the neutral EU phase ( $-1 < EU < 1$ ).

The relationship between the EU teleconnection pattern and winter precipitation in China is very close (Li and Chou, 1990). The reason is that the change in EU in winter is closely related to the atmospheric circulation across East Asia. In the positive EU phase in winter, the associated East Asian atmospheric circulation anomalies are as follows: the intensification of the high-level jet and the deepening of the trough in East Asia result in a stronger winter monsoon and lower temperature in East Asia, resulting in a lower temperature and less precipitation in East China. In contrast, in the negative EU phase in winter, the temperature rises, and the precipitation across eastern China increases. Hence, during the boreal winter, cooling and less precipitation are likely to occur in most of eastern China associated with the positive EU phase (Liu and Chen, 2012).

#### 4.5 Reasons for more precipitation in EE type

To illustrate the characteristics of the EE type, we plot the pressure and wind fields and precipitation (Figure 8). The EE-type pressure field is characterized by a low in the south and a high in the north (Figure 8 (a)), which leads to an anomalously strong easterly airflow into southeastern China. The warm moist air associated with this anomalously strong low-level easterly airflow likely contributes to precipitation in the EE type. Thus, the EE type generates the highest precipitation in southeastern China (Figure 8 (b)), due to the low-level jet just offshore carrying moisture from eastern China. Anomalously negative zonal winds (strong easterlies) at 850 hPa have been associated with precipitation.

Figure 8. (a) Mean sea level pressure (MSLP) anomalies (shaded; hPa) and 850 hPa wind patterns (vectors; m/s) of the EE type; (b) precipitation pattern derived from the EE type (shaded; mm/d) and 850 hPa wind pattern (vectors; m/s) of the EE type.

In winter, regardless of whether the winter monsoon is strong or weak, the coastal area of China's mainland from the middle latitude to the low latitude is controlled by the Mongolian high. The meridional tropism of the wind direction is very significant. When the EE type occurs, the winter monsoon decreases, and the wind vector transforms into a latitudinal vector. Thus, the wind direction is close to east (especially in the 5-20°N), and the northerly wind is much weaker. This situation is very beneficial to precipitation generation, and in fact, our results also confirm this observation.

It is worth noting that the combination of multiple WTs can affect precipitation differently compared to just one WT, indicating that one should not simply use a certain WT to anticipate the impacts associated with the combination of multiple WTs. The change of EE type includes not only the change of frequency, but also the change of structure. The relative frequency of each type is different each year. EE type is a combination of several types, and its frequency changes accordingly. Because the proportion of various types used to synthesize EE type will change every year, the structure of EE type is not the same every year. Therefore, change of EE type can not be estimated simply according to the change of a certain original type.

The EE type occurs more in the positive WP phase and in the negative EU phase (Figure 7). WP and EU were negatively correlated in winter. When WP is in the positive phase, EU is in the negative phase. At this time, the Mongolian high-pressure system weakened, and the southeastern part of China was at the intersection of high- and low-pressure systems (Figure 8). At the same time, the prevailing easterly wind due to the positive WP phase can transport enough water vapour from the ocean (Figure 8). All these factors provide favourable conditions for precipitation in southeastern China.

Taking all of this into account, the winter monsoon (northerly wind) from Mongolia Siberia high prevails in Southeast China in winter. The northerly wind comes from the inland area, and the weather is mainly sunny when it is controlled. However, if there is a short period of warm air (east wind) activity, it will form a front, and the east wind from the ocean will bring wet water vapor, so it is easy to produce precipitation. This is the case of EE type in this paper. From the perspective of local area, when EE type appears, it is mainly east wind. The cold and warm air meet and the east wind from the ocean can bring water vapor, which is easy to produce precipitation. From the perspective of larger scale teleconnection, EE type mainly appears in the positive phase of WP and the negative phase of EU, which provides a strong support for the explanation of the physical origin of more precipitation in EE type.

## 5. Summary and conclusion

We used the JC method to classify the MSLP data (1979-2005) across southeastern China, and classification results of 27 WTs were obtained. The results show that the JC classification method is suitable for southeastern China. These WTs have clear physical meanings and can describe the weather characteristics of southeastern China in winter, which provides a basis for the analysis of the relationship between the WT and precipitation.

To select the most precipitation-prone WTs in winter in southeastern China, a set of indicators describing precipitation and extreme precipitation were analysed. It was found that all WTs with an easterly wind component were prone to precipitation. There are 9 types (ANE, NE, CNE, AE, E, CE, ASE, SE, and CSE) containing easterly wind components, which are combined into one class named the EE type, for further analysis. In winter, the easterly wind can bring abundant water vapour to the southeastern part of China, which provides precipitation generation conditions.

We analysed the persistence and transformation characteristics of the top 10 most frequently occurring types. The EE type was found to be relatively persistent and is the easiest to convert from an anticyclone.

Accepted Article

Finally, we analysed the relationship between the WTs and teleconnections. We found that the EE type is more likely to appear in the positive WP phase and in the negative EU phase, which is consistent with the precipitation analysis results. This finding implies that the WP and EU influence precipitation conditions in this region through modulation of the occurrence of the EE type, which is also easy to explain on a large scale. These results will be useful for prediction of rainfall conditions.

The difference between this study and other studies is that we can predict whether the current weather pattern will produce precipitation by only judging the wind direction without analysing the state of other weather elements. This result has an important practical application value.

### Acknowledgements

This work was supported by the China Postdoctoral Science Foundation (Grant No. 2018M632334) and the Radar Imaging and Microwave Photonic Technology Key Laboratory of the Ministry of Education Grant. The NCEP/NCAR data were provided by the NOAA-CIRES Climate Diagnostics Center, Boulder, Colorado, USA (<http://www.cdc.noaa.gov>). The set of gridded precipitation data was provided by Chen *et al.* (<http://rcg.gvc.gu.se/data/ChinaPrecip>).

### References

- Agel L, Barlow M, Qian J H, Colby, F, Douglas, E, Eichler, T. 2015. Climatology of daily precipitation and extreme precipitation events in the northeast United States. *J. Hydrometeorol.* **16**(6): 2537-2557. doi:10.1175/jhm-d-14-0147.1.
- Belleflamme A, Fettweis X, Ericum M. 2015. Do global warming induced circulation pattern changes affect temperature and precipitation over Europe during summer? *Int. J. Climatol.* **35**:1484–1499.

- Chen D, Ou T, Gong L, Xu, C Y, Li, W, Ho, C H, Qian, W. 2010. Spatial interpolation of daily precipitation in China: 1951–2005. *Adv. Atmos. Sci.* **27**(6): 1221-1232. doi:10.1007/s00376-010-9151-y.
- Coleman JS, Rogers JC. 2007. A synoptic climatology of the central United States and associations with Pacific teleconnection pattern frequency. *J. Clim.* **20**(14):3485–3497.
- Conway D, Jones P D. 1998. The use of weather types and air flow indices for GCM downscaling. *J. Hydrol.* **212**: 348-361. doi:10.1016/s0022-1694(98)00216-9.
- Demuzere M, Werner M, Van Lipzig N P M, Roeckner, E. 2009. An analysis of present and future ECHAM5 pressure fields using a classification of circulation patterns. *Int. J. Climatol.* **29**(12): 1796-1810. doi:10.1002/joc.1821.
- Donat M G, Leckebusch G C, Pinto J G, Ulbrich, U. 2010. Examination of wind storms over Central Europe with respect to circulation weather types and NAO phases. *Int. J. Climatol.* **30**(9): 1289-1300. doi:10.1002/joc.1982.
- Huth R. 2000. A circulation classification scheme applicable in GCM studies. *Theor. Appl. Climatol.* **67**: 1-18.
- Huth R, Beck C, Kučerová M. 2016. Synoptic-climatological evaluation of the classifications of atmospheric circulation patterns over Europe. *Int. J. Climatol.* **36**(7): 2710-2726. doi:10.1002/joc.4546.
- Jenkinson A F, Collison F P, 1977. An initial climatology of gales over the North Sea. Synoptic climatology branch memorandum. **62**: Meteorological Office, Bracknell.
- Jiang, N. 2011. A new objective procedure for classifying New Zealand synoptic weather types during 1958–2008. *Int. J. Climatol.* **31**:863–879. doi:10. 1002/joc.2126.
- Jiang N, Griffiths G, Lorrey A. 2012. Influence of large-scale climate modes on New Zealand synoptic weather

types. *Int. J. Climatol.* **33**: 499–519. DOI: 10.1002/joc.3443.

Jiang, N., Cheung, K., Luo, K., Beggs, P. J., & Zhou, W. 2012. On two different objective procedures for classifying synoptic weather types over east Australia. *Int. J. Climatol.* **32**: 1475–1494. doi:10.1002/joc.2373.

Jiang, N., Luo, K., Beggs, P. J., Cheung, K., Scorgie, Y. 2015. Insights into the implementation of synoptic weather-type classification using self-organizing maps: an Australian case study. *Int. J. Climatol.* **35**: 3471–3485. doi:10.1002/joc.4221.

Jones P D, Hulme M, Briffa K R. 1993. A comparison of Lamb circulation types with an objective classification scheme. *Int. J. Climatol.* **13**(6): 655-663. doi:10.1002/joc.3370130606.

Jones PD, Harpham C, Briffa KR. 2013. Lamb weather types derived from reanalysis products. *Int. J. Climatol.* **33**:1129–1139.

Kanamitsu M, Ebisuzaki W, Woollen J, Yang, S K, Hnilo, J J, Fiorino, M, Potter, G L. 2002. NCEP–DOE AMIP-II reanalysis (R-2). *Bull. Am. Meteorol. Soc.* **83**(11): 1631-1644. doi:10.1175/bams-83-11-1631.

Lamb HH. 1972. British Isles weather types and a register of daily sequence of circulation patterns, 1861–1971. Geophysical Memoirs 116. Great Britain Meteorological Office. H. M. Stationary Office, London.

Li W, Chou J. 1990. Relation between monthly mean circulation in the northern hemisphere and the summer precipitation in the middle and lower reaches of Changjiang River. *Science Meteorologica Sinica.* **10**(2): 139-146. (in Chinese)

Li Y, He J, Jiang A. 2007. Circulation structure features of western pacific teleconnection pattern in winter and their relation with China's temperature and precipitation in winter. *Scientia Meteorologica Sinica.* **27**(2): 119-125. (in Chinese)

- Liu Y, Chen W. 2012. Variability of the Eurasian teleconnection pattern in the Northern Hemisphere winter and its influences on the climate in China. *Chinese Journal of Atmospheric Sciences*. **36**(2): 423-432. (in Chinese)
- Moron V, Robertson A W, Ward M N, Ndiaye, O. 2008. Weather types and rainfall over Senegal. Part I: Observational analysis. *J. Climate*. **21**(2): 266-287. doi:10.1175/2007jcli1601.1.
- Otero N, Sillmann J, Butler T. 2017. Assessment of an extended version of the Jenkinson-Collison classification on CMIP5 models over Europe. *Clim. Dyn.* **50**(5-6): 1559-1579. doi:10.1007/s00382-017-3705-y.
- Perez J, Menendez M, Mendez F J, Losada, I J. 2014. Evaluating the performance of CMIP3 and CMIP5 global climate models over the north-east Atlantic region. *Clim. Dyn.* **43**(9-10): 2663-2680. doi:10.1007/s00382-014-2078-8.
- Post P, Truija V, Tuulik J. 2002. Circulation weather types and their influence on temperature and precipitation in Estonia. *Boreal. Environ. Res.* **7**:281-289.
- Qian J H, Robertson A W, Moron V. 2010. Interactions among ENSO, the monsoon, and diurnal cycle in rainfall variability over Java, Indonesia. *J. Atmos. Sci.* **67**(11): 3509-3524. doi:10.1175/2010jas3348.1.
- Riddle E E, Stoner M B, Johnson N C, L'Heureux, M L, Collins, D C, Feldstein, S B. 2013. The impact of the MJO on clusters of wintertime circulation anomalies over the North American region. *Clim. Dyn.* **40**(7-8): 1749-1766. doi:10.1007/s00382-012-1493-y.
- Riediger U, Gratzkil A. 2014. Future weather types and their influence on mean and extreme climate indices for precipitation and temperature in Central Europe. *Meteorol. Z.* **23**(3):231-252.
- Roller C D, Qian J H, Agel L, Barlow, M, Moron, V. 2016. Winter weather regimes in the northeast United States.

*J. Climate*. **29**(8): 2963-2980. doi:10.1175/jcli-d-15-0274.1.

Sarricolea P, Meseguer-Ruiz, Oliver, Martín-Vide, Javier, et al. 2018. Trends in the frequency of synoptic types in central-southern Chile in the period 1961–2012 using the Jenkinson and Collison synoptic classification. *Theoretical & Applied Climatology*, **134**(1-2):193-204. doi: 10.1007/s00704-017-2268-5.

Shi N, Lu J. 1995. April northern 500 hPa mean field teleconnection patterns with their relation to rainfall in China. *Journal of Nanjing Institute of Meteorology*. **18**(3): 324-330. (in Chinese)

Spellman G. 2017. An assessment of the Jenkinson and Collison synoptic classification to a continental mid-latitude location. *Theor. Appl. Climatol.* **128**(3-4): 731-744. doi:10.1007/s00704-015-1711-8.

Straus D M, Corti S, Molteni F. 2007. Circulation regimes: Chaotic variability versus SST-forced predictability. *J. Climate*. **20**(10): 2251-2272. doi:10.1175/jcli4070.1.

Wallace J M, Gutzler D S. 1981. Teleconnections in the geopotential height field during the Northern Hemisphere winter. *Mon. Weather. Rev.* **109**(4): 784-812. doi:10.1175/1520-0493(1981)109<0784:titghf>2.0.co;2.

Yarnal B, Comrie A C, Frakes B, Brown, D P. 2001. Developments and prospects in synoptic climatology. *Int. J. Climatol.* **21**(15): 1923-1950. doi:10.1002/joc.675.

Zhu Y, Chen D, Li W, Zhang P. 2007. Lamb-Jenkinson circulation type classification system and its application in China. *Journal of Nanjing Institute of Meteorology*. **30**(3): 289-297. (in Chinese)

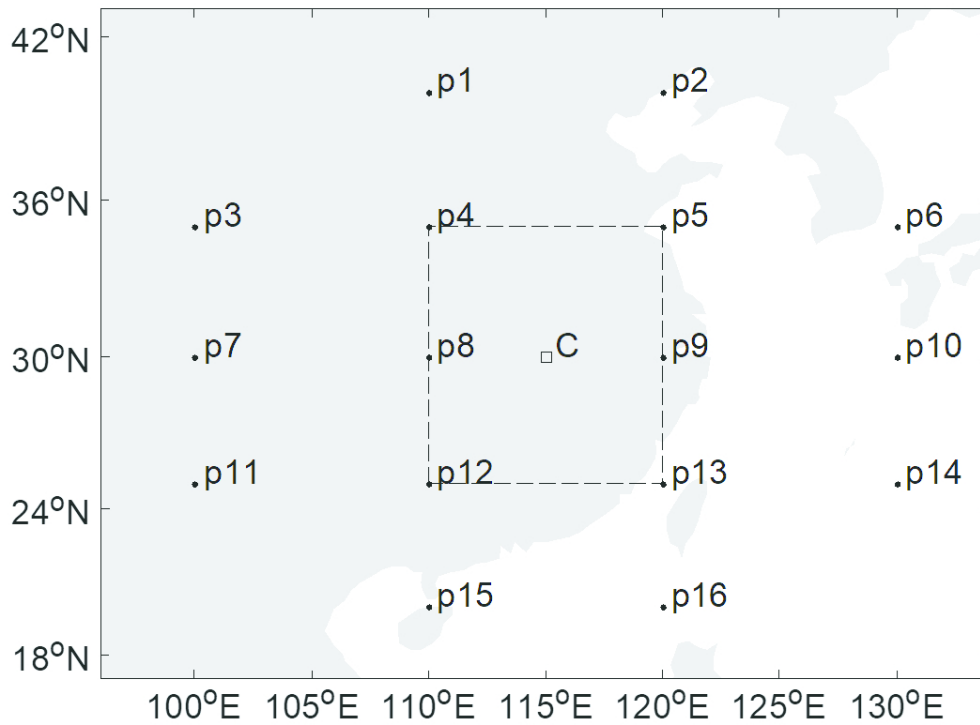


Figure 1. Map showing the boundaries of southeastern China used for JC classification and the core domain (the rectangle inside the larger rectangle). The 16 grid points generated via a distribution algorithm around the central point (square) located in southeastern China were likewise plotted.

375x274mm (72 x 72 DPI)

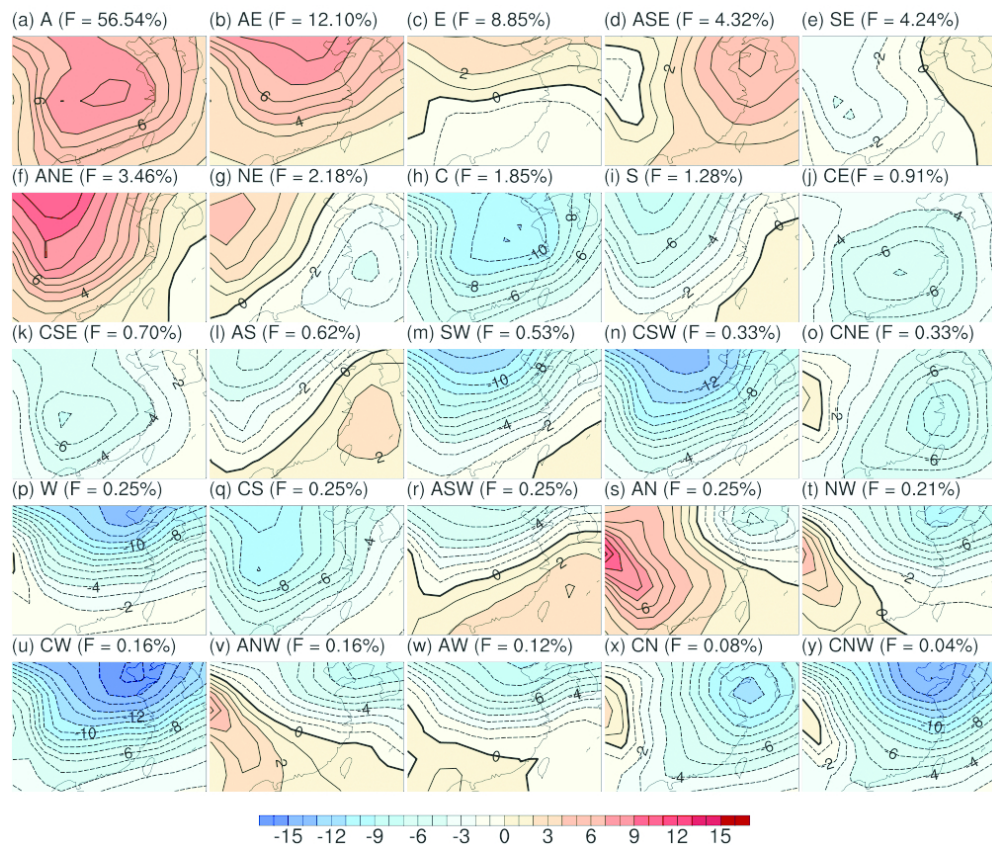


Figure 2. Weather types: mean sea level pressure (MSLP) anomalies (contour; hPa) for winter (DJF) 1979-2005. The subgraphs are ranked from high to low according to the frequency of occurrence. The frequency (F) of each class is also shown in brackets in the subgraphs. The MSLP anomalies were calculated by subtracting the averaged MSLP over the 27-yr baseline period from the daily MSLP at each grid point for the NCEP2 MSLP data.

216x182mm (119 x 119 DPI)

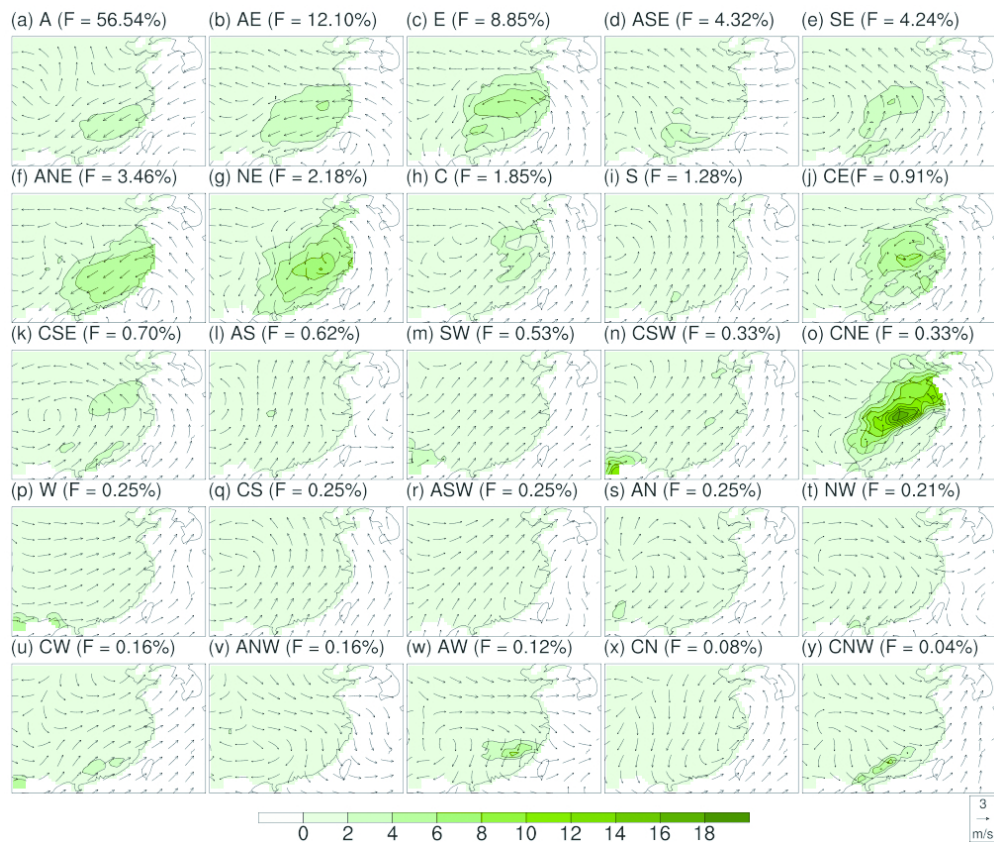


Figure 3. Precipitation and wind patterns derived from the weather types (corresponding to Figure 2): precipitation (PR) (shaded; mm/d) and 850hPa wind anomalies (vectors) for winter (DJF) from 1979-2005.

215x181mm (119 x 119 DPI)

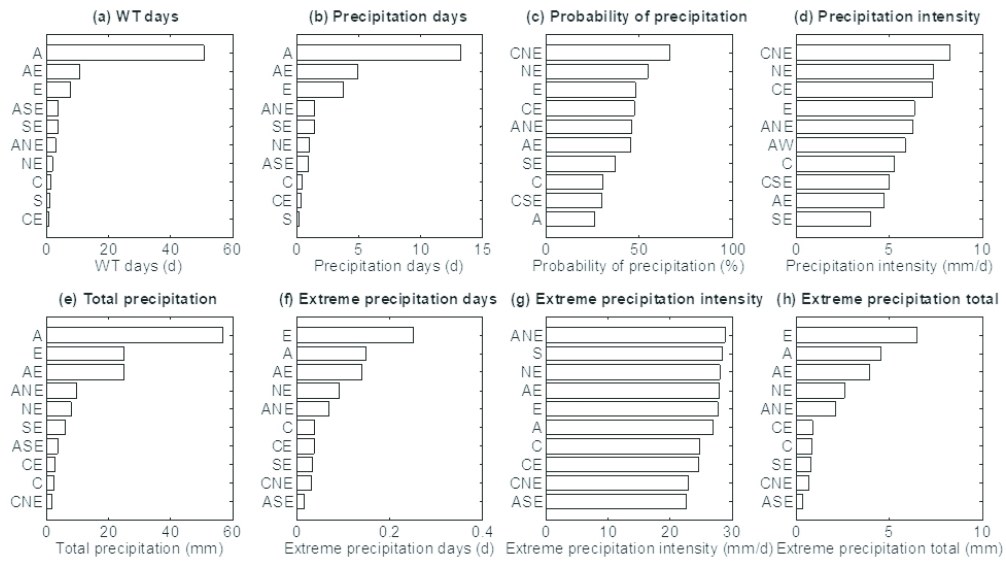


Figure 4. Mean precipitation characteristics (top 10) in the core domain for winter (DJF) from 1979-2005.

342x194mm (72 x 72 DPI)

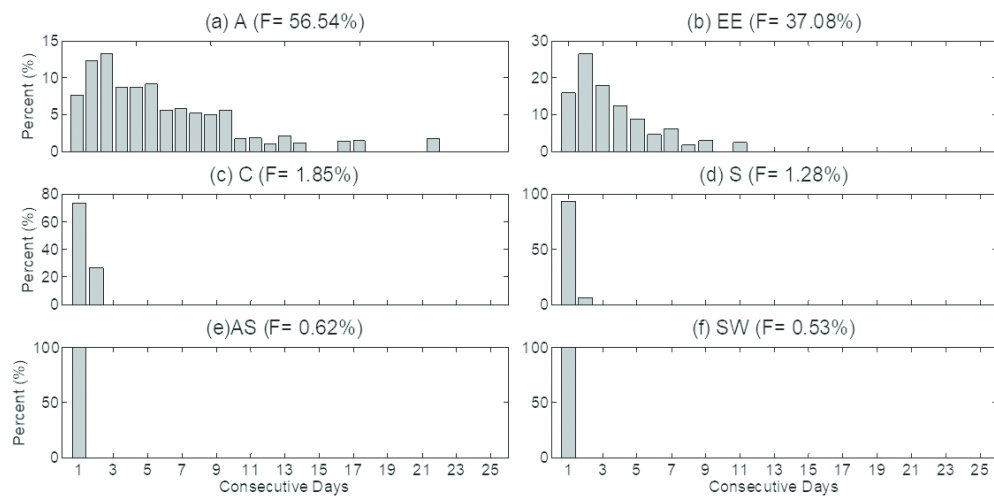


Figure 5. Persistence of WTs (a) A, (b) EE, (c) C, (d) S, (e) AS, and (f) SW (in winter), expressed as a percentage of the total WT days, for a duration of 1-25 days. The weather types that occur less frequently (frequency < 0.5%) are not shown.

398x195mm (72 x 72 DPI)

	A	EE	C	S	AS	SW	CSW	W	CS	ASW
A	998	294	7	20	15	9	2	2	2	5
EE	363	518	7	5	0	1	1	1	1	1
C	2	34	6	1	0	0	0	0	2	0
S	0	18	10	1	0	0	1	0	0	0
AS	0	11	1	0	0	2	0	0	1	0
SW	0	5	3	1	0	0	2	2	0	0
CSW	1	2	2	2	0	0	1	0	0	0
W	0	1	2	0	0	1	1	0	0	0
CS	0	2	4	0	0	0	0	0	0	0
ASW	0	5	1	0	0	0	0	0	0	0

Figure 6. Graphical representation of the progression and persistence of the top 10 WTs.

293x305mm (72 x 72 DPI)

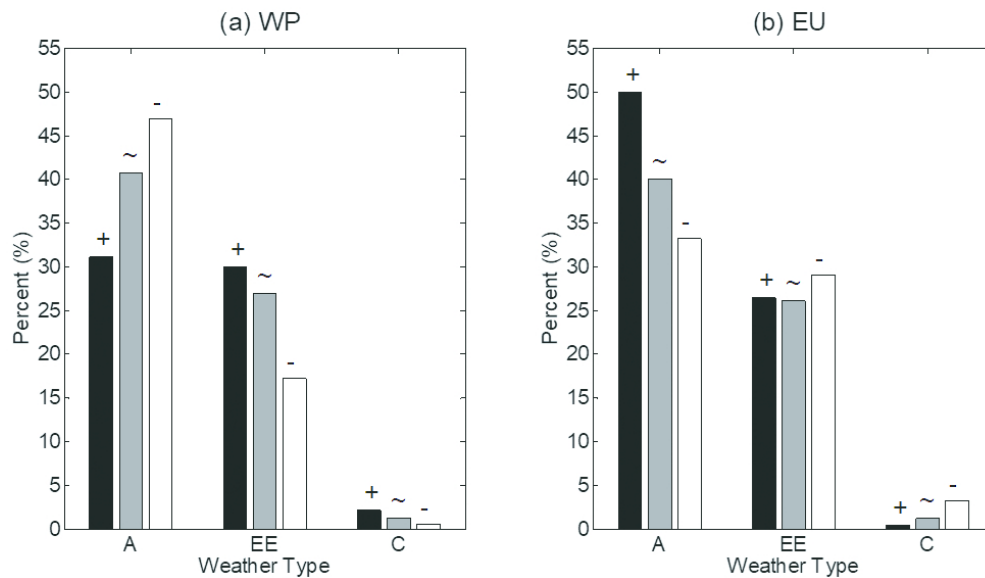


Figure 7: WT occurrence frequency during the three phases (positive (+), neutral (~) and negative (-) phases of (a) WP and (b) EU in winter. For each WT, the three bars represent the occurrence frequency during the three phases of the teleconnection pattern. Each bar represents the percentage of the same phase of each teleconnection. The frequencies of the other WTs are particularly low and are not shown in the figure. For each WT, the three bars represent the frequency during the three phases of the teleconnection pattern. Each bar represents the percentage of the same phase of each teleconnection.

345x198mm (72 x 72 DPI)

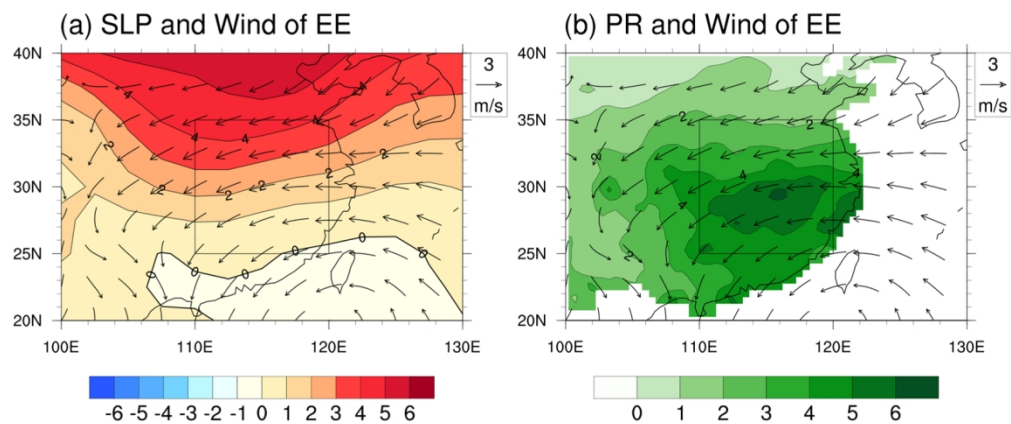


Figure 8. (a) Mean sea level pressure (MSLP) anomalies (shaded; hPa) and 850hPa wind patterns (vectors; m/s) of the EE type; (b) precipitation pattern derived from the EE type (shaded; mm/d) and 850hPa wind pattern (vectors; m/s) of the EE type.

Table 1. The number of the top 10 of the precipitation index rankings in winter. The maximum value is expressed in bold.

Classification included	WT days	Probability			Extreme precipitation days	Extreme precipitation intensity	Extreme precipitation total	
		Precipitation days	of precipitation	Precipitation intensity				
1 Anticyclonic components	4	4	3	3	4	4	4	
2 Cyclonic components	2	2	4	4	3	3	3	
3 Easterly components	7	7	<b>8</b>	<b>8</b>	<b>8</b>	<b>8</b>	7	<b>8</b>
4 Westerly components	0	0	0	1	0	0	0	
5 Southerly components	3	3	2	2	2	2	2	
6 Northerly components	2	2	3	3	3	3	3	